Effect of RF Filtering on the Performance of Uncoded PCM/PM Telemetry Channels

M. A. Koerner
Telecommunications Systems Section

This article describes a method for calculating the increase in received telemetry signal power required to compensate for the use of a radio frequency interference (RFI) filter in front of the DSN receiving system low-noise amplifier. The telemetry system for which the degradation is calculated is an uncoded PCM/PM system in which the NRZ data directly modulates the carrier at a modulation level which leaves a discrete carrier. A phase-locked loop in the RF receiver tracks the discrete carrier and coherently demodulates the PCM data. The RFI filter may be a series of Butterworth, Tchebychev, or Bessel low-pass, high-pass, band-pass, or band-reject filters, each with arbitrary bandwidth, number of poles, and, for band-pass or band-reject filters, resonant frequency. The only restriction is that the RFI filter must have only simple poles. Numerical results are presented for the RFI filters the DSN plans to place in front of the S-band FET, S-band maser, and X-band maser low noise amplifiers. The main conclusion is that the filters will produce negligible degradation at data rates below 4 Mbps.

I. Introduction

In conjunction with the Networks Consolidation Program (NCP), the DSN is developing band-pass filters to be placed in front of the S-band FET (field-effect transistor) low-noise amplifier (LNA) and the S-band and X-band maser LNAs. The purpose of these filters is to avoid LNA saturation by out-of-band radio frequency interference (RFI) signals. The DSN itself produces some of this interference, such as that from the DSN transmitters. The remainder comes from other systems operating in adjacent frequency bands. Reference 1 reports the results of a study to define the requirements for these filters.

The use of band-reject filters has also been considered. Such filters could be used to eliminate both in-band and out-of-band RFI signals that have fixed frequency and narrow bandwidth.

An unavoidable consequence of the use of these filters will be the degradation in telemetry performance caused by the telemetry signal distortion produced by these filters. The term "telemetry degradation" as used in this report is the increase in received signal power necessary to compensate for the addition of the RFI filter. Thus, the degradation will depend on the basis (i.e., bit error probability) on which telemetry performance is measured. The degradation will be greatest for very wide-band telemetry channels operating near the edge of the RFI filter pass-band. The objective of this analysis is (1) to develop a method of calculating this telemetry degradation for a variety of RFI filters, and (2) to apply this method to the RFI filters being developed by the DSN.

The telemetry system considered in this report is an uncoded PCM/PM system. A very simplified block diagram of this system is shown in Fig. 1. NRZ (non-return-to-zero) data directly phase modulates the RF carrier at a modulation level which leaves a discrete carrier component. At the DSN, a phase-locked loop in the RF receiver, which follows the RFI filter and LNA, tracks the received carrier and demodulates

the uncoded NRZ PCM signal. The RF receiver is followed by an integrate-and-dump circuit, which integrates the RF receiver output over one bit time. A bit synchronizer establishes the timing for the integrate-and-dump circuit. At the end of the integration time for each bit, a binary decision is made as to whether a PCM "0" or "1" was transmitted, based on the polarity of the integrate-and-dump circuit output.

The primary alternatives to the telemetry system analyzed in this report are (1) an uncoded PCM/PM system where the carrier is completely suppressed and a Costas loop recovers the carrier reference, and (2) an uncoded PCM/PSK/PM system where the NRZ PCM data phase shift keys a subcarrier and the resulting signal phase modulates the carrier. While some work was done on both of these systems, it was decided to concentrate on the discrete carrier PCM/PM system because this is the system most likely to be used, at least initially, by the DSN for the very wideband telemetry channels for which significant degradation is expected from signal distortion in the RFI filter.

While this analysis considers only uncoded PCM/PM channels, it would be desirable to analyze systems such as Viterbi or Reed-Solomon/Viterbi channels, where the raw data are coded and the resulting coded symbol stream phase modulates the carrier. However, with the exception of Manchester coding, to which the results obtained herein can be easily extended, an analysis for coded channels, similar to that presented here for uncoded channels, does not appear feasible. Note, however, that the results presented here are equally valid for coded channels, as long as the channel symbol error probability is used as the measure of telemetry channel performance and the probability of symbol sequences in the coded PCM is the same as that in random data.

This analysis employs two important approximations. First, the analysis assumes that the RF receiver phase-locked loop tracks the received carrier with some constant phase error ϕ. The RF receiver phase-lock loop phase errors caused by thermal noise and the portion of the telemetry sidebands that fall within the bandwidth of the RF receiver phase-locked loop are neglected. Thus, any interaction between the signal distortion caused by the RFI filter and the time-varying RF receiver phase-locked loop phase error will not be uncovered by this analysis. Second, this analysis does not determine the actual displacement in bit synchronizer bit timing caused by the signal distortion. The analysis supplies a method of calculating the degradation as a function of the displacement in bit synchronizer timing. A first estimate of the displacement in bit synchronizer timing is made using the slope at zero frequency of the phase response of the RFI filter's baseband equivalent, and the telemetry degradation is calculated for this bit timing. This timing displacement will be that seen by very narrowband telemetry channels. Then, using this estimate of bit synchronizer timing displacement as an initial value, the bit synchronizer timing which minimizes the telemetry degradation and the degradation for this bit synchronizer timing is calculated. The actual bit synchronizer timing displacement may not be at the optimum value. Of course, it would always be possible to manually adjust bit synchronizer timing to the optimum value, but this may not be practical for normal telemetry operations.

II. Analysis

The objective of this analysis is to provide a method of computing the telemetry channel performance degradation caused by the RFI filter. Each of the subsections into which this section is divided provides the equations necessary for one step in the computational process. Because of the complexity of the problem, no attempt will be made to analytically combine the results presented in these subsections.

A. RFI Filter Poles and Residues

A basic assumption of this analysis is that the RFI filter has only simple poles. The transfer function of such a filter can be expressed in the form

$$H(s) = Q_0 + \sum_{k=1}^{N} \frac{Q_k}{s - P_k} \tag{1}$$

where Q_0 is the filter response at infinite frequency, P_k is the kth pole of the filter, and Q_k is the residue at that pole. The first step in calculating the telemetry degradation caused by the RFI filter is to calculate the response at infinity and the poles and residues for the RFI filter.

This article considers an RFI filter consisting of an arbitrary number of cascaded elements. Since the RFI filter has only simple poles, each of its elements must have only simple poles and therefore a transfer function of the form shown in Eq. (1). Each of these elements can be a Butterworth, Tchebychev, or Bessel low-pass filter or the high-pass, band-pass, or band-reject filters which can be synthesized from these low-pass filters using simple frequency transformations. Thus, this analysis provides the capability for assessing the telemetry degradation produced by using both a band-pass RFI filter for rejection of out-of-band RFI and one or more band-reject filters for eliminating in-band RFI.

The first step in calculating the RFI filter response at infinity, its poles, and the residues at these poles, is to calculate these parameters for the low-pass equivalent of each RFI filter element. The response at infinity and the poles and residues for RFI filter elements that are high-pass, band-pass,

or band-reject filters will be calculated from the response at infinity and the poles and residues of these low-pass equivalents. The low-pass equivalent's frequency response will be adjusted to have unit response at zero frequency and either amplitude response A at some frequency $f_A = (2\pi)^{-1}\,\omega_A$ or noise bandwidth B_N and will have zero response at infinite frequency. The transfer functions of the Butterworth, Tchebychev, and Bessel low-pass filters considered in this article have no zeros. Therefore, if $P_0, \ldots, P_N$ are the poles of the low-pass equivalent, the residue at the kth pole will be

$$Q_k = -P_k \prod_{\substack{\ell=1 \\ \ell \neq k}}^{N} \left(1 - \frac{P_k}{P_\ell}\right)^{-1} \tag{2}$$

1. Butterworth low-pass filters. The poles of a Butterworth low-pass filter with N poles will be

$$P_k = -\omega_B \sin\left[(2k-1)\frac{\pi}{2N}\right] - i\omega_B \cos\left[(2k-1)\frac{\pi}{2N}\right], \quad 1 \leqslant k \leqslant N \tag{3}$$

where $f_B = (2\pi)^{-1}\omega_B$ is the half-power bandwidth of the low-pass filter. f_B can be calculated from f_A and A or from B_N using

$$f_B = (A^{-2} - 1)^{-1/2N} f_A \tag{4}$$

or

$$f_B = B_N \sin\frac{\left(\frac{\pi}{2N}\right)}{\left(\frac{\pi}{2N}\right)} \tag{5}$$

2. Tchebychev low-pass filters. The poles of a Tchebychev low-pass filter with N poles will be located at

$$P_k = -\omega_T \sinh\left[N^{-1}\sinh^{-1}(\epsilon^{-1})\right]\sin\left[(2k-1)\frac{\pi}{2N}\right] - i\omega_T \cosh\left[N^{-1}\sinh^{-1}(\epsilon^{-1})\right]\cos\left[(2k-1)\frac{\pi}{2N}\right], \quad 1 \leqslant k \leqslant N \tag{6}$$

where $f_T = (2\pi)^{-1}\omega_T$ is the cut-off frequency of the Tchebychev filter and

$$\epsilon = (\rho^{-2} - 1)^{1/2} \tag{7}$$

where $20 \log_{10}(\rho)$ is the Tchebychev filter ripple factor. When f_A is specified, f_T can be computed using

$$f_T = \frac{1}{\cosh\left\{N^{-1}\cosh^{-1}\left[\epsilon^{-1}(A^{-2}-1)^{1/2}\right]\right\}} f_A, \quad N = \text{odd}$$

$$= \frac{1}{\cosh\left\{N^{-1}\cosh^{-1}\left[\epsilon^{-1}(A^{-2}(1+\epsilon^2)-1)^{1/2}\right]\right\}} f_A, \quad N = \text{even} \tag{8}$$

When B_N is specified, the poles and residues, P'_k and Q'_k, $1 \leqslant k \leqslant N$, of a Tchebychev filter with unit cutoff frequency ($f_T = 1$) are calculated. Then the poles and residues of the desired filter are

$$P_k = \frac{B_N}{B'_N} P'_k, \quad 1 \leqslant k \leqslant N \tag{9}$$

and

$$Q_k = \frac{B_N}{B'_N} Q'_k, \quad 1 \leqslant k \leqslant N \tag{10}$$

where

$$B'_N = -\frac{1}{4}\sum_{k=1}^{N}\left(\frac{Q'_k}{P'_k}\right)^2 - \sum_{k=1}^{N}\sum_{\ell=1}^{k-1}\left(\frac{Q'_k\,Q'_\ell}{P'_k + P'_\ell}\right) \tag{11}$$

is the noise bandwidth of the Tchebychev filter with unit cutoff frequency.

3. Bessel low-pass filter. An N-pole Bessel low-pass filter with unit response at zero frequency has transfer function

$$H_{LP}(s) = \frac{a_{NO}}{p_N(cs)} \tag{12}$$

where

$$p_N(s) = \sum_{k=0}^{N} a_{Nk}\, s^k \tag{13}$$

is the Nth order Bessel polynomial and c is a parameter which is adjusted to give either the required bandwidth f_A at attenuation A or the required noise bandwidth B_N. The Nth order Bessel polynomial is defined by the recursion formula

$$p_N(s) = (2N-1)p_{N-1}(s) + s^2 p_{N-2}(s) \tag{14}$$

where $p_0(s) = 1$ and $p_1(s) = s + 1$. The corresponding recursion relationships for the Bessel polynomial coefficients are

$$a_{N0} = (2N-1)\, a_{N-1,0} \tag{15}$$

$$a_{N1} = (2N-1)\, a_{N-1,1} \tag{16}$$

$$a_{Nk} = (2N-1)\, a_{N-1,k} + a_{N-2,k-2}, \qquad 2 \leqslant k \leqslant N-1 \tag{17}$$

and

$$a_{NN} = A_{N-2,N-2} \tag{18}$$

Used recursively, Eq. (12) and Eqs. (15) through (18) provide a simple method of calculating (for $c = 1$) the coefficients in the transfer function of a Bessel filter of any number of poles.

When f_A and A are specified, one first adjusts c to obtain the desired bandwidth and then employs a polynomial root funding subroutine to calculate the filter poles (the roots of $p_N(cs)/a_{N0}$). First, one finds the frequency $f'_A = (2\pi)^{-1}\omega'_A$ at which $|a_{N0}/p_N(s)|$ is equal to A. This is equivalent to finding the zero of

$$I(\omega) = 1 - A^2\left\{\left[1 + \sum_{\substack{k=2 \\ k=\text{even}}}^{N} (-1)^{k/2}\, \frac{a_{Nk}}{a_{N0}}\, \omega^k\right]^2 + \left[\sum_{\substack{k=1 \\ k=\text{odd}}}^{N} (-1)^{(k-1)/2}\, \frac{a_{Nk}}{a_{N0}}\, \omega^k\right]^2\right\} \tag{19}$$

This can be solved using a series of linear extrapolations. To use this method an expression for $I'(\omega) = dI(\omega)/d\omega$ is needed. Differentiating Eq. (19),

$$I'(\omega) = -2A^2\left\{\left[1 + \sum_{\substack{k=2 \\ k=\text{even}}}^{N} (-1)^{k/2}\, \frac{a_{Nk}}{a_{N0}}\, \omega^k\right] \times \left[\sum_{\substack{k=2 \\ k=\text{even}}}^{N} (-1)^{k/2}\, \frac{a_{Nk}}{a_{N0}}\, k\omega^{k-1}\right] + \left[\sum_{\substack{k=1 \\ k=\text{odd}}}^{N} (-1)^{(k-1)/2}\, \frac{a_{Nk}}{a_{N0}}\, \omega^k\right] \times \left[\sum_{\substack{k=1 \\ k=\text{odd}}}^{N} (-1)^{(k-1)/2}\, \frac{a_{Nk}}{a_{N0}}\, k\omega^{k-1}\right]\right\} \tag{20}$$

Having determined ω'_A such that $I(\omega'_A) = 0$,

$$c = \frac{\omega'_A}{\omega_A} \tag{21}$$

When the noise bandwidth B_N is specified, a polynomial root-funding subroutine can be used to calculate the poles P'_K, $1 \leqslant k \leqslant N$, of $a_{N0}/p_N(s)$. Then, the residues Q'_k of $a_{N0}/p_N(s)$ at these poles can be calculated using P'_K instead of P_K in Eq. (2). Finally, Eqs. (9), (10) and (11) above can be used to calculate the poles and residues of a Bessel filter with the desired noise bandwidth.

4. High-pass filters. A high-pass filter can be synthesized from a low-pass filter using the transformation

$$H_{HP}(s) = H_{LP}\left(\frac{\omega_A^2}{s}\right) \tag{22}$$

If the low-pass filter has unit response at zero frequency, amplitude response A at frequency f_A, and zero response at infinite frequency, the high-pass filter will have zero response at zero frequency, amplitude response A at frequency f_A, and unit response at infinite frequency. If P_K and Q_K are the poles and residues of the low-pass filter, the response at infinity of the high-pass filter is

$$Q'_0 = -\sum_{k=1}^{N} \frac{Q_k}{P_k} \tag{23}$$

The location of the kth pole of the high-pass filter will be

$$P'_k = \frac{\omega_A^2}{P_k} \tag{24}$$

and the residue at that pole will be

$$Q'_k = -\frac{\omega_A^2}{P_k^2} Q_k \tag{25}$$

5. Band-pass filters. A band-pass filter can be synthesized from a low-pass filter using the transformation

$$H_{BP} = H_{LP}\left(s + \frac{\omega_R^2}{s}\right) \tag{26}$$

where $f_R = (2\pi)^{-1}\omega_R$ is the band-pass filter resonant frequency. The resonant frequency will be approximately equal to the filter center frequency. If the low-pass filter has unit response at zero frequency and zero response at infinite frequency, the band-pass filter will have zero response at zero frequency, unit response at f_R, and zero response at infinite frequency. Furthermore, if the low-pass filter has attenuation A at frequency f_A, the band-pass filter will have bandwidth f_A between points at which the band-pass filter attenuation is A.

If P_K and Q_K, $1 \leqslant k \leqslant N$, are the poles and residues of the low-pass filter, the response at infinity of the band-pass filter will be zero and the band-pass filter poles will be

$$P'_k = \frac{1}{2} P_k + i\omega_R \left[1 - \left(\frac{P_k}{2\omega_R}\right)^2\right]^{1/2}, \quad 1 \leqslant k \leqslant N \tag{27}$$

and

$$P''_k = \frac{1}{2} P_k - i\omega_R \left[1 - \left(\frac{P_k}{2\omega_R}\right)^2\right]^{1/2}, \quad 1 \leqslant k \leqslant N \tag{28}$$

Note that the band-pass filter has $2N$ poles. The residues at these poles will be

$$Q'_k = Q_k \left(1 - \frac{P''_k}{P'_k}\right)^{-1} \tag{29}$$

and

$$Q''_k = Q_k \left(1 - \frac{P'_k}{P''_k}\right)^{-1} \tag{30}$$

6. Band-reject filters. A band-reject filter can be synthesized from a low-pass filter using the transformation

$$H_{BR}(s) = H_{LP}\left[\omega_A^2 \left(s + \frac{\omega_R^2}{s}\right)^{-1}\right] \tag{31}$$

If the low-pass filter has unit response at zero frequency and zero response at infinite frequency, the band-reject filter will have unit response at zero frequency, zero response at f_R, and unit response at infinite frequency. Furthermore, if the low-pass filter has attenuation A at frequency f_A, the band-reject filter will have bandwidth f_A between points at which the band-reject filter attenuation is A.

If P_K and Q_K, $1 \leqslant k \leqslant N$, are the poles and residues of the low-pass filter, the response at infinity of the band-reject filter will be

$$Q'_0 = -\sum_{k=1}^{N} \frac{Q_k}{P_k} \tag{32}$$

and the band-reject filter poles will be

$$P'_k = \frac{\omega_A^2}{2P_k} + i\omega_R \left[1 - \left(\frac{\omega_A^2}{2P_k\omega_R}\right)^2\right]^{1/2}, \quad 1 \leqslant k \leqslant N \tag{33}$$

and

$$P''_k = \frac{\omega_A^2}{2P_k} - i\omega_R \left[1 - \left(\frac{\omega_A^2}{2P_k\omega_R}\right)^2\right]^{1/2}, \quad 1 \leqslant k \leqslant N \tag{34}$$

Note that the band-reject filter has $2N$ poles. The residues at these poles will be

$$Q'_k = -\frac{\omega_A^2}{P_k^2} Q_k \left(1 - \frac{P''_k}{P'_k}\right)^{-1} \tag{35}$$

and

$$Q''_k = -\frac{\omega_A^2}{P_k^2} Q_k \left(1 - \frac{P'_k}{P''_k}\right)^{-1} \tag{36}$$

7. Cascaded elements. Having developed equations for calculating the response at infinity, the poles, and the residues at these poles for the individual elements of the RFI filter, the next step is to calculate the response at infinity, the poles, and the residues at these poles for the combination of a series of such elements. Consider two filters, one with N_1 poles and another with N_2 poles, which have no common pole. Let Q_{01} be the response at infinity and P_{1K} and Q_{1K} be the poles and residues of the first filter and Q_{02} be the response at infinity and P_{2K} and Q_{2K} be the poles and residues for the second filter. The cascade of the two filters has $N_1 + N_2$ poles, P_{1K}, $1 \leqslant k \leqslant N_1$, and P_{2K}, $1 \leqslant k \leqslant N_2$. The response at infinity of the cascaded filter will be

$$Q_0' = Q_{01} Q_{02} \tag{37}$$

The cascaded filter residue at P_{1K} will be

$$Q_{1k}' = Q_{1k} \left[Q_{02} + \sum_{\ell=1}^{N_2} \frac{Q_{2\ell}}{P_{1k} - P_{2\ell}} \right] \tag{38}$$

and that at P_{2K} will be

$$Q_{2k}' = Q_{2k} \left[Q_{01} + \sum_{\ell=1}^{N_1} \frac{Q_{1\ell}}{P_{2k} - P_{1\ell}} \right] \tag{39}$$

Starting with two RFI filter elements, the above process can be repeated until the response of the RFI filter at infinity, the RFI filter poles, and the residues at these poles have been calculated.

B. RF Receiving System

Figure 2 shows the analytical model for the demodulation of the telemetry data signal from the RF carrier. Note that noise is introduced at two different locations in Fig. 2. $n_0(t)$ represents the noise, such as atmospheric and antenna noise, introduced prior to the RFI filter. $n_2(t)$ represents the noise, such as the FET or maser LNA noise, introduced after the RFI filter. Two noise sources are required because the RFI filter will reduce the effective telemetry detector noise bandwidth for noise introduced prior to the RFI filter, but not for noise introduced after the RFI filter. The analysis assumes that the one-sided power spectral densities of $n_0(t)$ and $n_2(t)$ are $(1 - \eta)N_0$ and ηN_0 where N_0 is the one-sided power spectral density of the receiving system noise produced by all sources and η, $0 \leqslant \eta \leqslant 1$, is the fraction of this noise introduced after the RFI filter.

Referring again to Fig. 2, the signal and noise components of the RFI filter input will be

$$s_0(t) = (2P)^{1/2} \sin [\omega_C t + \phi_C + \beta x(t)] \tag{40}$$

and

$$n_0(t) = n_{0I}(t)\, 2^{1/2} \sin (\omega_C t + \phi_C - \phi) + n_{0Q}(t)\, 2^{1/2} \cos (\omega_C t + \phi_C - \phi) \tag{41}$$

P is the received signal power, $f_C = (2\pi)^{-1}\omega_C$ is the carrier frequency, and ϕ_C is the carrier phase. β is the telemetry modulation level and $x(t)$ is the binary-valued (± 1) telemetry modulation. This analysis assumes $\overline{x(t)}$ is zero. $n_{0I}(t)$ and $n_{0Q}(t)$ are statistically independent gaussian processes with constant one-sided power spectral density $(1 - \eta)N_0$ over the frequency band occupied by the telemetry data signal. Note that for analytical convenience the quadrature noise components of $n_0(t)$ are referenced to a carrier with instantaneous phase $\omega_C t + \phi_C - \phi$, where ϕ is the static phase error in the RF receiver phase-locked loop.

For the input signal and noise specified in Eqs. (40) and (41), the signal and noise output of an RFI filter with impulse response $h(t)$, amplitude response $A(\omega)$, and phase response $\phi(\omega)$ will be

$$\begin{aligned} s_1(t) = {} & (2P)^{1/2} \cos(\beta) A(\omega_C) \sin [\omega_C t + \phi_C + \phi(\omega_C)] \\ & + (2P)^{1/2} \sin(\beta) \cos [\omega_C t + \phi_C + \phi(\omega_C)] \\ & \times \int_0^\infty h_C(\tau)\, x(t - \tau)\, d\tau \\ & + (2P)^{1/2} \sin(\beta) \sin [\omega_C t + \phi_C + \phi(\omega_C)] \\ & \times \int_0^\infty h_S(\tau)\, x(t - \tau)\, d\tau \end{aligned} \tag{42}$$

and

$$n_1(t) = 2^{1/2} \sin [\omega_C t + \phi_C + \phi(\omega_C) - \phi]$$

$$\times \int_0^\infty h_C(\tau)\, n_{0I}(t-\tau)\, d\tau$$

$$- 2^{1/2} \cos [\omega_C t + \phi_C + \phi(\omega_C) - \phi]$$

$$\times \int_0^\infty h_S(\tau)\, n_{0I}(t-\tau)\, d\tau$$

$$+ 2^{1/2} \cos [\omega_C t + \phi_C + \phi(\omega_C) - \phi]$$

$$\times \int_0^\infty h_C(\tau)\, n_{0Q}(t-\tau)\, d\tau$$

$$+ 2^{1/2} \sin [\omega_C t + \phi_C + \phi(\omega_C) - \phi]$$

$$\times \int_0^\infty h_S(\tau)\, n_{0Q}(t-\tau)\, d\tau \qquad (43)$$

where

$$h_C(\tau) = h(\tau) \cos [\omega_C \tau + \phi(\omega_C)] \qquad (44)$$

and

$$h_S(\tau) = h(\tau) \sin [\omega_C \tau + \phi(\omega_C)] \qquad (45)$$

The noise $n_2(t)$ introduced after the RFI filter will have the form

$$n_2(t) = n_{2I}(t)\, 2^{1/2} \sin [\omega_C t + \phi_C + \phi(\omega_C) - \phi]$$

$$+ n_{2Q}(t)\, 2^{1/2} \cos [\omega_C t + \phi_C + \phi(\omega_C) - \phi] \qquad (46)$$

where, as in Eq. (41), the carrier instantaneous phase to which the quadrature noise components are referenced is chosen for analytical convenience.

Assuming the RF receiver phase-locked loop tracks the carrier component of the RFI filter output with phase error ϕ, the reference signal for carrier demodulation shown in Fig. 2 will be

$$s_3(t) = 2^{1/2} \cos [\omega_C t + \phi_C + \phi(\omega_C) - \phi] \qquad (47)$$

Thus, neglecting terms with zero frequency and terms in $2\omega_C t$, the signal and noise outputs of the carrier demodulator will be

$$s_4(t) = P^{1/2} \sin (\beta) \int_0^\infty [h_C(\tau) \cos (\phi)$$

$$+ h_S(\tau) \sin (\phi)]\, x(t-\tau)\, d\tau \qquad (48)$$

and

$$n_4(t) = n_{2Q}(t) + \int_0^\infty h_C(\tau)\, n_{0Q}(t-\tau)\, d\tau$$

$$- \int_0^\infty h_S(\tau)\, n_{0I}(t-\tau)\, d\tau \qquad (49)$$

Using the above results, Fig. 3 shows a simplified analytical model for the DSN RF receiving system and telemetry detector. The transfer functions $H'(s)$, $H_C(s)$, and $H_S(s)$ shown in Fig. 3 are those corresponding to the impulse responses $h'(\tau)$, $h_C(\tau)$, and $h_S(\tau)$ where

$$h'(\tau) = h_C(\tau) \cos (\phi) + h_S(\tau) \sin (\phi) \qquad (50)$$

For an RFI filter having a transfer function of the form shown in Eq. (1),

$$H_C(s) = Q_{C0} + \sum_{k=1}^{N} \frac{Q_{Ck}}{s - P_{Ck}} \qquad (51)$$

and

$$H_S(s) = Q_{S0} + \sum_{k=1}^{N} \frac{Q_{Sk}}{s - P_{Sk}} \qquad (52)$$

where

$$P_{Ck} = P_{Sk} = P_k - i\omega_C, \quad Im(P_k) > 0$$
$$= P_k + i\omega_C, \quad Im(P_k) < 0 \tag{53}$$

where $Im(z)$ denotes the imaginary part of a complex variable z,

$$Q_{Ck} = \frac{1}{2} Q_k \exp[-i\phi(\omega_C)], \quad Im(P_k) > 0$$
$$= \frac{1}{2} Q_k \exp[+i\phi(\omega_C)], \quad Im(P_k) < 0 \tag{54}$$

$$Q_{Sk} = -\frac{1}{2i} Q_k \exp[-i\phi(\omega_C)], \quad Im(P_k) > 0$$
$$= \frac{1}{2i} Q_k \exp[i\phi(\omega_C)], \quad Im(P_k) < 0 \tag{55}$$

$$Q_{C0} = Q_0 \cos[\phi(\omega_C)] \tag{56}$$

and

$$Q_{S0} = Q_0 \sin[\phi(\omega_C)] \tag{57}$$

Thus,

$$H'(s) = Q_0' + \sum_{k=1}^{N} \frac{Q_k'}{S - P_k'} \tag{58}$$

where

$$P_k' = P_{Ck} = P_{Sk}, \quad 1 \leq k \leq N \tag{59}$$

and

$$Q_k' = Q_{Ck} \cos(\phi) + Q_{Sk} \sin(\phi), \quad 0 \leq k \leq N \tag{60}$$

Equations (53) through (57) and Eqs. (59) and (60) provide a means of calculating the response at infinity and the poles and residues of the transfer functions $H'(s)$, $H_C(s)$, and $H_S(s)$ shown in Fig. 3, given the response at infinity and the poles and residues of the RFI filter.

The effect of the *noise* filtering shown in Fig. 3 on telemetry system performance will be to increase telemetry performance by $1/\delta_N$ where δ_N is the factor by which the variance of the noise at the integrate-and-dump circuit output is reduced by the filtering. The next section of this report provides a means of calculating the ratio of the bandwidth of an integrate-and-dump circuit preceded by a filter with only simple poles to that of the integrate-and-dump circuit alone. Thus, if δ_{NC} is this ratio for the filter with transfer function $H_C(s)$ and δ_{NS} is this ratio for the filter with transfer function $H_S(s)$,

$$\delta_N = \eta + (1 - \eta)(\delta_{NC} + \delta_{NS}) \tag{61}$$

Thus, as expected, if all of the receiving system noise is introduced after the RFI filter, $\eta = 1$ and $\delta_N = 1$. When the noise is introduced after the RFI filter, the RFI filter does not reduce the effect of the noise on telemetry performance.

C. Reduction in the Telemetry Detector Noise Bandwidth Produced by a Filter Preceding the Integrate-and-Dump Circuit

As discussed in the preceding section, a method is needed for calculating the reduction in telemetry detector noise bandwidth caused by a filter with only simple poles preceding the integrate-and-dump circuit. Since the filter has only simple poles, its impulse response will have the form

$$h_1(\tau) = Q_0 \delta(\tau) + \sum_{k=1}^{N} Q_k \exp(P_k \tau) \tag{62}$$

where Q_0 is the filter response at infinite frequency, P_K and Q_k, $1 \leq k \leq N$, are the filter poles and residues, and $\delta(\tau)$ is the Dirac delta function. The impulse response of the integrate-and-dump circuit will be

$$h_2(\tau) = 1, \quad 0 \leq \tau \leq T,$$
$$= 0, \quad \tau > T \tag{63}$$

where T is the integration time. The impulse response of the cascaded filters will be the convolution of $h_1(t)$ and $h_2(t)$ or

$$h(\tau) = Q_0 + \sum_{k=1}^{N} \frac{Q_k}{P_k} [\exp(P_k \tau) - 1], \quad 0 \leq \tau \leq T$$
$$= \sum_{k=1}^{N} \frac{Q_k}{P_k} [1 - \exp(-P_k T)] \exp(P_k \tau), \quad T \leq \tau \leq \infty \tag{64}$$

The one-sided noise bandwidth of a filter with impulse response $h(\tau)$ will be

$$B_N = \frac{1}{2} \int_0^\infty h^2(\tau)\, d\tau \tag{65}$$

The noise bandwidth of the integrate-and-dump circuit above is $T/2$. Thus, using Eq. (64) in Eq. (65), the reduction in noise bandwidth caused by the filtering in front of the integrate-and-dump circuit will be

$$\frac{B_N}{T/2} = \left(Q_0 - \sum_{k=1}^{N} \frac{Q_k}{P_k}\right)^2 + 2 \sum_{k=1}^{N} \frac{Q_k}{P_k} \frac{\exp(P_k T) - 1}{P_k T} \left(Q_0 - \sum_{\ell=1}^{N} \frac{Q_\ell}{P_k + P_\ell}\right) \tag{66}$$

Having computed the response at infinity and the poles and residues for the transfer functions $H_C(s)$ and $H_S(s)$, using the equations derived in the previous section, Eq. (66) with appropriate substitutions, can be used to calculate δ_{NC} and δ_{NS}.

D. Probability Density of the Integrate-and-Dump Circuit Output Signal Level

As a result of the filter with transfer function $H'(s)$ shown in Fig. 3, the signal integrated by the integrate-and-dump circuit will depend not only on the data bit being detected, but also on preceding bits and, in this analysis, on one succeeding bit. The dependence on preceding bits occurs because the impulse response of $H'(s)$ will, in general, be of infinite duration; that is, the current output of $H'(s)$ depends on all previous inputs. The dependence on the succeeding bit is a consequence of the displacement in bit synchronizer timing caused by $H'(s)$. This analysis assumes the displacement in bit synchronizer timing does not exceed one bit.

Each different signal waveform that can occur during a bit integration can result in a different integrate-and-dump circuit output signal level. This analysis assumes that the impulse response of $H'(s)$ is significant for only M bit times. If the impulse response extends over M preceding bits, and one succeeding bit is significant because of bit synchronizer timing displacement, there are 2^{M+2} possible integrate-and-dump circuit output levels. This analysis assumes that all data sequences occur with equal probability. Hence, all of the 2^{M+2} possible integrate-and-dump circuit output signal levels occur with equal probability $1/2^{M+2}$.

The next step is to calculate each of the 2^{M+2} possible output signal levels. Refer to the simplified block diagram in Fig. 4 and the sample $x(t)$ waveform in Fig. 5. Note that the nth data bit in $x(t)$ is received during $[(\lambda + n - 1)T, (\lambda + n)T]$. Assume that because of the distortion of $x(t)$ the bit synchronizer causes the integrate-and-dump circuit to integrate over $[(\hat{\lambda} + n - 1)T, (\hat{\lambda} + n)T]$, during detection of the nth data bit, where $\hat{\lambda} = \lambda + \epsilon$. Then

$$z_n = \int_{(\lambda+n-1+\epsilon)T}^{(\lambda+n+\epsilon)T} y(t)\, dt \tag{67}$$

or

$$z_n = \int_{(\lambda+n-1+\epsilon)T}^{(\lambda+n)T} y(t)\, dt + \int_{(\lambda+n)T}^{(\lambda+n+\epsilon)T} y(t)\, dt, \qquad 0 \leqslant \epsilon \leqslant 1 \tag{68}$$

and

$$z_n = \int_{(\lambda+n-1+\epsilon)T}^{(\lambda+n-1)T} y(t)\, dt + \int_{(\lambda+n-1)T}^{(\lambda+n+\epsilon)T} y(t)\, dt, \qquad -1 \leqslant \epsilon \leqslant 0 \tag{69}$$

If $h'(\tau)$, the impuse response corresponding to the transfer function $H'(s)$, has the form

$$h'(\tau) = Q_0 \delta(\tau) + \sum_{k=1}^{N} Q_k \exp(P_k \tau) \tag{70}$$

$$y(t) = x_n \sum_{k=1}^{N} \frac{Q_k}{P_k} [\exp\{P_k [t - (\lambda + n - 1)T]\} - 1] + \sum_{m=-\infty}^{n-1} x_m \sum_{k=1}^{N} \frac{Q_k}{P_k} \times [\exp\{P_k [t - (\lambda + m - 1)T]\} - \exp\{P_k [t - (\lambda + m)T]\}], \quad (\lambda + n - 1)T \leqslant t \leqslant (\lambda + n)T \tag{71}$$

Using Eq. (71) in Eqs. (68) and (69),

$$z_n = \sum_{m=-1}^{\infty} c_m x_{n-m}, \qquad x_{n-m} = \pm 1 \tag{72}$$

where

$$c_0 = (1-\epsilon)\left[Q_0 - \sum_{k=1}^{N}\frac{Q_k}{P_k}\right] + \sum_{k=1}^{N}\frac{Q_k}{P_k^2 T}\{\exp[(1+\epsilon)P_k T] - 2\exp(\epsilon P_k T) + 1\}, \quad 0 \leqslant \epsilon \leqslant 1 \tag{73}$$

$$c_0 = (1+\epsilon)\left[Q_0 - \sum_{k=1}^{N}\frac{Q_k}{P_k}\right] + \sum_{k=1}^{N}\frac{Q_k}{P_k^2 T}\{\exp[(1+\epsilon)P_k T] - 1\}, \quad -1 \leqslant \epsilon \leqslant 0 \tag{74}$$

$$c_{-1} = \epsilon\left[Q_0 - \sum_{k=1}^{N}\frac{Q_k}{P_k}\right] + \sum_{k=1}^{N}\frac{Q_k}{P_k^2 T}[\exp(\epsilon P_k T) - 1], \quad 0 \leqslant \epsilon \leqslant 1 \tag{75}$$

$$c_{-1} = 0, \quad -1 \leqslant \epsilon \leqslant 0 \tag{76}$$

$$c_1 = \sum_{k=1}^{N}\frac{Q_k}{P_k^2 T}\{\exp[(2+\epsilon)P_k T] - 2\exp[(1+\epsilon)P_k T] + \exp(\epsilon P_k T)\}, \quad 0 \leqslant \epsilon \leqslant 1 \tag{77}$$

$$c_1 = -\epsilon\left[Q_0 - \sum_{k=1}^{N}\frac{Q_k}{P_k}\right] + \sum_{k=1}^{N}\frac{Q_k}{P_k^2 T}\{\exp[(2+\epsilon)P_k T] - 2\exp[(1+\epsilon)P_k T] + 1\}, \quad -1 \leqslant \epsilon \leqslant 0 \tag{78}$$

and

$$c_m = \sum_{k=1}^{N}\frac{Q_k}{P_k^2 T}\{\exp[(m+1+\epsilon)P_k T] - 2\exp[(m+\epsilon)P_k T] + \exp[(m-1+\epsilon)P_k T]\}, \quad -1 \leqslant \epsilon \leqslant 1, m \geqslant 2 \tag{79}$$

Thus, approximating the infinite summation in Eq. (72) with one whose upper limit is M, the probability density function of the integrate-and-dump circuit output signal level, normalized to $P^{1/2}\sin(\beta)$, is

$$p(z_n) = \frac{1}{2^{M+2}}\sum_{x_{n-M}=\pm 1}\cdots\sum_{x_{n+1}=\pm 1} \times \delta\left(z_n - \sum_{m=-1}^{M} x_{n-m}c_m\right) \tag{80}$$

E. Telemetry Performance Degradation

Having determined the probability density function of the integrate-and-dump circuit output signal level and the reduction in the noise bandwidth of the telemetry detector, it remains to calculate the telemetry performance degradation. In a system with no filter or RF receiver phase error ($\phi = 0$), the channel bit error probability will be

$$P_B = \frac{1}{2}\left\{1 - Erf\left[\left(\frac{E_B}{N_0}\right)^{1/2}\right]\right\} \tag{81}$$

where E_B is the received signal energy per bit and N_0 is the receiving system noise spectral density. In such a system, z_n and δ_N will be one. When z_n and δ_N are not one, the effect on the bit error probability is equivalent to that of reducing $(E_B/N_0)^{1/2}$ by $z_N/\delta_N^{1/2}$. Therefore, in the presence of signal distortion and RF receiver phase error, the bit error probability will be

$$P_B = \frac{1}{2^{M+1}}\sum_{\mathbf{x}}\frac{1}{2}\left\{1 - Erf\left[\left(\frac{E_B}{N_0}\cdot\frac{1}{\delta_N}\right)^{1/2}(\mathbf{x}\cdot\mathbf{c})\right]\right\} \tag{82}$$

$\mathbf{x}$ is the vector $(x_{n-M}, \ldots, x_{n-1}, 1, x_{n+1})$, $\mathbf{c}$ is the vector $(c_M, \ldots, c_{-1})$, $\mathbf{x} \cdot \mathbf{c}$ is the dot product of the two vectors, and

$$\sum_{\mathbf{x}}$$

denotes the summation over all the 2^{M+1} possible values of x. Note that to simplify the above analysis (without any loss of generality) the nth transmitted bit was assumed to be a binary zero ($x_n = 1$). If P_B is the allowable telemetry channel bit error probability and $(E_B/N_0)_B$ is the E_B/N_0 that yields this bit error probability in the absence of filtering and RF receiver phase error, the telemetry channel performance degradation δ_T will be the solution of

$$P_B = \frac{1}{2^{M+1}} \sum_{\mathbf{x}} \frac{1}{2} \left[1 - Erf \left\{ \left[\left(\frac{E_B}{N_0} \right)_B \cdot \frac{\delta_T}{\delta_N} \right]^{1/2} (\mathbf{x} \cdot \mathbf{c}) \right\} \right] \tag{83}$$

This equation can be solved for δ_T using a series of linear extrapolations starting with some initial estimate for δ_T (i.e., $\delta_T = 1$). Since P_B will be almost an exponential function of δ_T, convergence of this iterative process will be accelerated by working with the natural logarithm $\ell n(x)$ of both sides of Eq. (83). Thus, the slope needed for the linear extrapolation will be

$$\frac{d\ell n(P_B)}{d\delta_T} = \frac{1}{P_B} \frac{dP_B}{d\delta_T} \tag{84}$$

where

$$\frac{dp_B}{d\delta_T} = -\frac{1}{2} \left[\frac{\left(\frac{E_B}{N_0} \right)_B}{\pi \delta_N \delta_T} \right]^{1/2}$$

$$\times \frac{1}{2^{M+1}} \sum_{\mathbf{x}} (\mathbf{x} \cdot \mathbf{c}) \exp \left[- \frac{\left(\frac{E_B}{N_0} \right)_B \delta_T}{\delta_N} (\mathbf{x} \cdot \mathbf{c})^2 \right] \tag{85}$$

F. Bit Synchronizer Timing Displacement

Examining Eqs. (82) and (83) and Eqs. (73) through (79), one notes that the telemetry channel bit error probability and the performance degradation δ_T will be a function of ϵ, the displacement in bit synchronizer timing expressed as a fraction of the bit time. While analytical prediction of the bit synchronizer timing displacement appears feasible, such an analysis would be quite difficult. In this report two alternate approaches are used.

1. Narrowband approximation. The first and simplest approach is to calculate an estimate of ϵ from the phase response of the filter with transfer function $H'(s)$ shown in Figs. 3 and 4. For narrowband telemetry modulation, the displacement in bit synchronizer timing will be equal to the time delay through $H'(s)$ at very low frequencies. Thus, if

$$H'(i\omega) = A'(\omega) \exp [i\phi'(\omega)] \tag{86}$$

the narrowband approximation to the displacement in bit synchronizer timing will be

$$\epsilon_I = \frac{1}{T} \frac{d\phi'(\omega)}{d\omega} \bigg|_{\omega=0} \tag{87}$$

If the response at infinity Q_0 and the poles and residues, P_k and Q_k $(1 \leqslant k \leqslant N)$ of $H'(s)$ are known, and

$$a_k = [R(P_k)]^2 + [I(P_k)]^2 \tag{88}$$

$$b_k = -2I(P_k) \tag{89}$$

$$c_k = -R(Q_k)R(P_k) - I(Q_k)I(P_k) \tag{90}$$

$$d_k = I(Q_k) \tag{91}$$

$$e_k = R(Q_k)I(P_k) - I(Q_k)R(P_k) \tag{92}$$

$$f_k = -R(Q_k) \tag{93}$$

where $R(z)$ and $I(z)$ denote the real and imaginary parts of a complex variable z,

$$\epsilon_I = \frac{1}{T} \frac{X(0)Y'(0) - Y(0)X'(0)}{[X(0)]^2 + [Y(0)]^2} \tag{94}$$

where

$$X(0) = Q_0 + \sum_{k=1}^{N} \frac{c_k}{a_k} \tag{95}$$

$$Y(0) = \sum_{k=1}^{N} \frac{e_k}{a_k} \tag{96}$$

$$X'(0) = \sum_{k=1}^{N} \frac{(a_k d_k - b_k c_k)}{a_k^2} \tag{97}$$

and

$$Y'(0) = \sum_{k=1}^{N} \frac{(a_k f_k - b_k e_k)}{a_k^2} \tag{98}$$

2. Bit synchronizer timing displacement for minimum telemetry degradation. The second and somewhat more complex approach is to find the bit synchronizer timing displacement which minimizes the telemetry performance degradation. If the bit synchronizer does not automatically adjust the timing to minimize the telemetry degradation, the timing could be manually adjusted to achieve the minimum performance degradation. Of course, requiring manual adjustment of bit synchronizer timing might create some operational difficulties.

A second iterative procedure, also using a series of linear extrapolations, can be employed to find the value of ϵ (ϵ_o) that minimizes δ_T. Finding the value of ϵ that minimizes δ_T is equivalent to finding the zero of $d\delta_T/d\epsilon$. To find a zero crossing of a function, the iterative process requires an initial estimate of the solution and a means of calculating the function and its derivative. The initial estimate used herein (ϵ_I) is that obtained using the narrowband approximation discussed above. $d\delta_T/d\epsilon$ and $d^2\delta_T/d\epsilon^2$ can be calculated using

$$\frac{d\delta_T}{d\epsilon} = -2\delta_T \frac{\alpha}{\beta} \tag{99}$$

and

$$\frac{d^2\delta_T}{d\epsilon^2} = -2\left[\frac{\alpha}{\beta}\frac{d\delta_T}{d\epsilon} + \frac{\delta_T}{\beta}\frac{d\alpha}{d\epsilon} - \frac{\delta_T \alpha}{\beta^2}\frac{d\beta}{d\epsilon}\right] \tag{100}$$

where

$$\alpha = \sum_{\mathbf{x}} \left(\mathbf{x} \cdot \frac{d\mathbf{c}}{d\epsilon}\right) \exp\left[-\frac{\delta_T}{\delta_N}\left(\frac{E_B}{N_0}\right)_B (\mathbf{x} \cdot \mathbf{c})^2\right] \tag{101}$$

$$\beta = \sum_{\mathbf{x}} (\mathbf{x} \cdot \mathbf{c}) \exp\left[-\frac{\delta_T}{\delta_N}\left(\frac{E_B}{N_0}\right)_B (\mathbf{x} \cdot \mathbf{c})^2\right] \tag{102}$$

$$\frac{d\alpha}{d\epsilon} = \sum_{\mathbf{x}} \left[\mathbf{x}\frac{d^2\mathbf{c}}{d\epsilon^2} - \frac{1}{\delta_N}\left(\frac{E_B}{N_0}\right)_B (\mathbf{x} \cdot \mathbf{c})^2 \left(\mathbf{x} \cdot \frac{d\mathbf{c}}{d\epsilon}\right)\frac{d\delta_T}{d\epsilon} - 2\frac{\delta_T}{\delta_N}\left(\frac{E_B}{N_0}\right)_B (\mathbf{x} \cdot \mathbf{c})\left(\mathbf{x} \cdot \frac{d\mathbf{c}}{d\epsilon}\right)^2\right] \times \exp\left[-\frac{\delta_T}{\delta_N}\left(\frac{E_B}{N_0}\right)_B (\mathbf{x} \cdot \mathbf{c})^2\right] \tag{103}$$

$$\frac{d\beta}{d\epsilon} = \sum_{\mathbf{x}} \left[\mathbf{x} \cdot \frac{d\mathbf{c}}{d\epsilon} - (\mathbf{x} \cdot \mathbf{c})^3 \frac{1}{\delta_N}\left(\frac{E_B}{N_0}\right)_B \frac{d\delta}{d\epsilon} - 2\frac{\delta_T}{\delta_N}\left(\frac{E_B}{N_0}\right)_B (\mathbf{x} \cdot \mathbf{c})^2 \left(\mathbf{x} \cdot \frac{d\mathbf{c}}{d\epsilon}\right)\right] \times \exp\left[-\frac{\delta_T}{\delta_N}\left(\frac{E_B}{N_0}\right)_B (\mathbf{x} \cdot \mathbf{c})^2\right] \tag{104}$$

$$\frac{d\mathbf{c}_0}{d\epsilon} = -\left[Q_0 - \sum_{k=1}^{N} \frac{Q_k}{P_k}\right] + \sum_{k=1}^{N} \frac{Q_k}{P_k}\{\exp[(1+\epsilon)P_k T] - 2\exp(\epsilon P_k T)\}, \quad 0 \leq \epsilon \leq 1 \tag{105}$$

$$\frac{d^2\mathbf{c}_0}{d\epsilon^2} = \sum_{k=1}^{N} Q_k T\{\exp[(1+\epsilon)P_k T] - 2\exp(\epsilon P_k T)\}, \quad 0 \leq \epsilon \leq 1 \tag{106}$$

$$\frac{dc_0}{d\epsilon} = Q_0 - \sum_{k=1}^{N} \frac{Q_k}{P_k} + \sum_{k=1}^{N} \frac{Q_k}{P_k} \exp\left[(1+\epsilon)P_k T\right], \quad -1 \leqslant \epsilon \leqslant 0 \tag{107}$$

$$\frac{d^2 c_0}{d\epsilon^2} = \sum_{k=1}^{N} Q_k T \exp\left[(1+\epsilon)P_k T\right], \quad -1 \leqslant \epsilon \leqslant 0 \tag{108}$$

$$\frac{dc_{-1}}{d\epsilon} = Q_0 - \sum_{k=1}^{N} \frac{Q_k}{P_k} + \sum_{k=1}^{N} \frac{Q_k}{P_k} \exp\left(\epsilon P_k T\right), \quad 0 \leqslant \epsilon \leqslant 1 \tag{109}$$

$$\frac{d^2 c_{-1}}{d\epsilon^2} = \sum_{k=1}^{N} Q_k T \exp\left(\epsilon P_k T\right), \quad 0 \leqslant \epsilon \leqslant 1 \tag{110}$$

$$\frac{dc_{-1}}{d\epsilon} = \frac{d^2 c_{-1}}{d\epsilon^2} = 0, \quad -1 \leqslant \epsilon \leqslant 0 \tag{111}$$

$$\frac{dc_1}{d\epsilon} = \sum_{k=1}^{N} \frac{Q_k}{P_k} \left\{\exp\left[(2+\epsilon)P_k T\right] - 2\exp\left[(1+\epsilon)P_k T\right] + \exp\left(\epsilon P_k T\right)\right\}, \quad 0 \leqslant \epsilon \leqslant 1 \tag{112}$$

$$\frac{d^2 c_1}{d\epsilon^2} = \sum_{k=1}^{N} Q_k T \left\{\exp\left[(2+\epsilon)P_k T\right] - 2\exp\left[(1+\epsilon)P_k T\right] + \exp\left(\epsilon P_k T\right)\right\}, \quad 0 \leqslant \epsilon \leqslant 1 \tag{113}$$

$$\frac{dc_1}{d\epsilon} = -\left[Q_0 - \sum_{k=1}^{N} \frac{Q_k}{P_k}\right] + \sum_{k=1}^{N} \frac{Q_k}{P_k} \left\{\exp\left[(2+\epsilon)P_k T\right] - 2\exp\left[(1+\epsilon)P_k T\right]\right\}, \quad -1 \leqslant \epsilon \leqslant 0 \tag{114}$$

$$\frac{d^2 c_1}{d\epsilon^2} = \sum_{k=1}^{N} Q_k T \left\{\exp\left[(2+\epsilon)P_k T\right] - 2\exp\left[(1+\epsilon)P_k T\right]\right\}, \quad -1 \leqslant \epsilon \leqslant 0 \tag{115}$$

$$\frac{dc_m}{d\epsilon} = \sum_{k=1}^{N} \frac{Q_k}{P_k} \left\{\exp\left[(m+1+\epsilon)P_k T\right] - 2\exp\left[(m+\epsilon)P_k T\right] + \exp\left[(m-1+\epsilon)P_k T\right]\right\}, \quad -1 \leqslant \epsilon \leqslant 1, m \geqslant 2 \tag{116}$$

$$\frac{d^2 c_m}{d\epsilon^2} = \sum_{k=1}^{N} Q_k T \left\{\exp\left[(m+1+\epsilon)P_k T\right] - 2\exp\left[(m+\epsilon)P_k T\right] + \exp\left[(m-1+\epsilon)P_k T\right]\right\}, \quad -1 \leqslant \epsilon \leqslant 1, m \geqslant 2 \tag{117}$$

III. Numerical Results

Data are presented in this section for the telemetry channel degradation for the S-band FET amplifier, S-band maser amplifier, and X-band maser amplifier RFI filters. For each of these RFI filters telemetry channel degradation is plotted as a function of the telemetry channel carrier frequency for telemetry channel data rates of 4 Mbps, 10 Mbps, and 20 Mbps. The 4 Mbps rate is the highest data rate currently planned. The data for the 10 Mbps and 20 Mbps data rates were included to show the impact of the RFI filters on future systems. Plotting the telemetry channel degradation as a function of carrier frequency shows the impact of the RFI filter on telemetry channels whose center frequency does not fall at the RFI filter center frequency.

Two sets of curves are shown for each RFI filter. One set assumes that all of the receiving system noise is introduced after the RFI filter ($\eta = 1$). The other set assumes that all of the receiving system noise is introduced before the RFI filter ($\eta = 0$). The telemetry degradation δ_{T1} that occurs when all the noise is introduced after the RFI filter will always be greater than the telemetry degradation δ_{T0} that occurs when all the noise is introduced after the RFI filter, because the RFI filter reduces the telemetry system noise bandwidth for noise introduced prior to the RFI filter. Given the two sets of data ($\eta = 1$ and $\eta = 0$) for each RFI filter, the telemetry degradation for any other value of η is

$$\delta_T = \frac{\delta_{T1}\,\delta_{T0}}{(1-\eta)\delta_{T1} + \eta\delta_{T0}} \tag{118}$$

A. S-band FET Amplifier RFI Filter

Figures 6 and 7 show the telemetry channel degradation as a function of carrier frequency for the S-band FET amplifier RFI filter. Figure 6 assumes all of the noise is introduced after the RFI filter ($\eta = 1$). Figure 7 assumes all of the noise is introduced prior to the RFI filter ($\eta = 0$). The results presented in Figs. 6 and 7 assume that the RF receiver phase-locked loop static phase error is zero and that the allowable telemetry channel bit error probability is 10^{-5}.

The data shown in Figs. 6 and 7 are for 7th and 9th order Tchebychev bandpass filters with 270 MHz bandwidth between points at which the filter attenuation is -70 dB and 0.01 dB ripple factor. The filter resonant frequency, which is approximately equal to the filter center frequency, is 2250 MHz.

The telemetry channel degradation shown in Figs. 6 and 7 increases significantly with data rate, even when the carrier frequency is at the center of the RFI filter passband. The degradation increases significantly as the edge of the passband is approached. While the filter amplitude response may cause significant degradation, it is suspected that much of the degradation shown in Figs. 6 and 7 results from the non-linear phase response of the Tchebychev filter. While the degradation shown in Figs. 6 and 7 for the 4 Mbps data rate, especially that for the 9th order filter, seems acceptable, it appears that the use of this filter will cause significant telemetry degradation at much higher bit rates. This degradation will be significant even for telemetry channels whose center frequency is at the RFI filter center frequency.

B. S-band Maser Amplifier RFI Filter

Figures 8 and 9 show the telemetry channel degradation as a function of carrier frequency for the S-band maser amplifier RFI filter. Figure 8 assumes that all of the noise is introduced after the RFI filter ($\eta = 1$). Figure 9 assumes all of the noise is introduced before the RFI filter ($\eta = 0$). The results presented in Figs. 8 and 9 assume the RF receiver phase-locked loop static phase error is zero and that the allowable telemetry channel bit error probability is 10^{-5}.

The data shown in Figs. 8 and 9 are for a 5th order Tchebychev bandpass filter with 60 MHz bandwidth between points at which the filter attenuation is -0.5 dB and 0.01 dB ripple factor. The filter resonant frequency is 2292 MHz.

As in the case of the S-band FET amplifier RFI filter, the telemetry channel degradation increases significantly with data rate, even when the carrier frequency is near the RFI filter center frequency. The telemetry degradation does not seem unreasonable for the current 4 Mbps maximum data rate, but the degradation at higher data rates may not be acceptable.

C. X-band Maser Amplifier RFI Filter

Figures 10 and 11 show the telemetry channel degradation as a function of carrier frequency for the X-band maser amplifier RFI filter. Figure 10 assumes that all of the noise is introduced after the RFI filter ($\eta = 1$). Figure 11 assumes that all of the noise is introduced before the RFI filter ($\eta = 0$). The results shown in Figs. 10 and 11 assume that the RF receiver phase-locked loop phase error is zero and that the allowable telemetry channel bit error probability is 10^{-5}.

The data shown in Figs. 10 and 11 are for a 5th order Tchebychev bandpass filter with 160 MHz bandwidth between the points at which the filter attenuation is -3 dB and either 0.01 or 0.05 dB ripple factor. The filter resonant frequency is 8450 MHz. The 0.05 dB ripple factor curves in Fig. 11 were omitted for the 4 and 10 Mbps data rates, because they were essentially the same as the 0.01 dB ripple factor curves for the corresponding cases.

As in the cases of the S-band FET amplifier RFI filter and the S-band maser amplifier RFI filter, the telemetry channel degradation increases significantly with data rate. However, the telemetry channel degradation caused by the X-band maser amplifier RFI filter seems to be appreciably less than that produced by the S-band RFI filters. For 4 Mbps the degradation for $\eta = 1$, the worst case, is less than 0.1 dB over essentially all of the 8400 to 8500 MHz frequency band. For 10 Mbps the degradation is less than 0.2 dB over almost all of this frequency band. Even at 20 Mbps, the degradation is only about 0.25 dB for a carrier located at the RFI filter center frequency. Finally, the Tchebychev filter ripple factor does not appear to strongly affect the telemetry channel degradation produced by the X-band maser amplifier RFI filter.

D. Effect of Bit Synchronizer Timing Displacement

As noted in Section II.F of this article, this analysis does not calculate the actual bit synchronizer timing displacement. The "narrowband" approximation is used to obtain an initial estimate of bit synchronizer timing displacement and then an iterative process is employed to find the bit synchronizer timing displacement that minimizes telemetry channel degradation. It is this minimum value of the telemetry channel degradation that is plotted in Figs. 6 through 11.

The assumption in plotting this minimum telemetry channel degradation is that bit synchronizer timing can always be manually adjusted to optimize performance. However, as manual adjustment of bit synchronizer timing may be very cumbersome, let us assess the impact of non-optimum bit synchronizer timing displacement by comparing both the initial estimate of bit synchronizer timing displacement, obtained using the narrowband approximation, with the optimum value of bit synchronizer timing displacement and the telemetry channel degradations for these two estimates of bit synchronizer timing displacement.

Figure 12 compares the initial estimate and optimum value of bit synchronizer timing displacement, and Fig. 13 compares the corresponding telemetry degradations as a function of carrier frequency for the S-band maser RFI filter. Clearly, for carrier frequencies near the edge of the RFI filter passband, there is a substantial difference between the initial estimate and the optimum value of bit synchronizer timing displacement and also a substantial difference between the degradations. The degradation for the initial estimate is significantly greater, for carrier frequencies near the edge of the RFI filter passband, than the minimum degradation. This suggests that the telemetry degradation could be somewhat greater than that shown in Figs. 6 through 11, if actual bit synchronizer timing displacement differs from the optimum value as much as the initial estimate does and manual adjustment is not feasible.

IV. Conclusion

This article has presented a method for determining the effects of telemetry channel filtering on the performance of a discrete carrier PCM/PM telemetry channel and has applied this technique to calculate numerical results for the S-band FET amplifier, S-band maser amplifier and X-band maser amplifier RFI filters being considered by the DSN. This method can be adapted to calculate telemetry channel degradation for a very wide variety of RFI filters. The method can be easily extended to filters other than the cascaded Butterworth, Tchebychev, and Bessel low-pass, high-pass and band-reject filters considered herein, as long as the RFI filter has only simple poles and its poles and the residues at these poles can be calculated.

The numerical results presented for the S-band FET amplifier, S-band maser amplifier, and X-band maser amplifier RFI filters show that the telemetry channel degradation should be negligible for bit rates less than the current 4 Mbps maximum capability of the BBA (baseband assembly) telemetry processor. However, at data rates significantly greater than 4 Mbps, the telemetry degradation produced by the RFI filters, especially the S-band RFI filters, may be unacceptable.

Reference

1. "Final RFI Report," Ford Aerospace and Communications Corporation, 12-7-81.

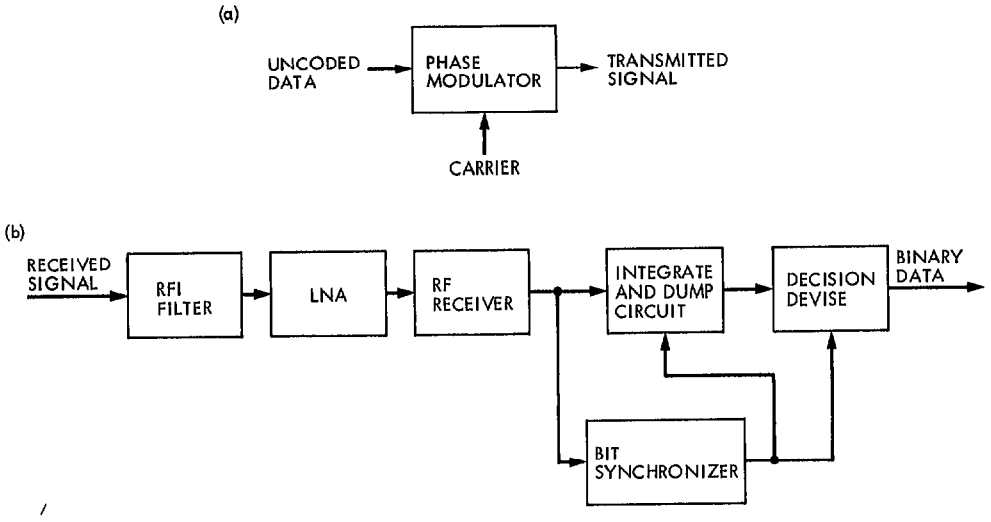

Fig. 1. Uncoded PCM/PM telemetry link block diagram: (a) transmitting system; (b) receiving system

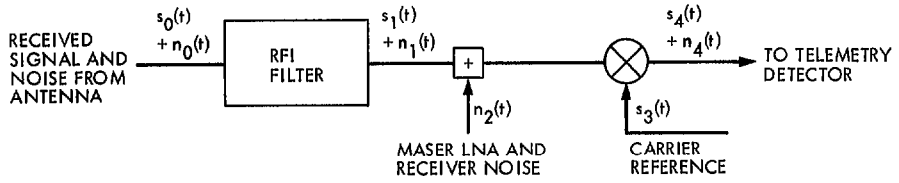

Fig. 2. Analytical model for the RF receiving system

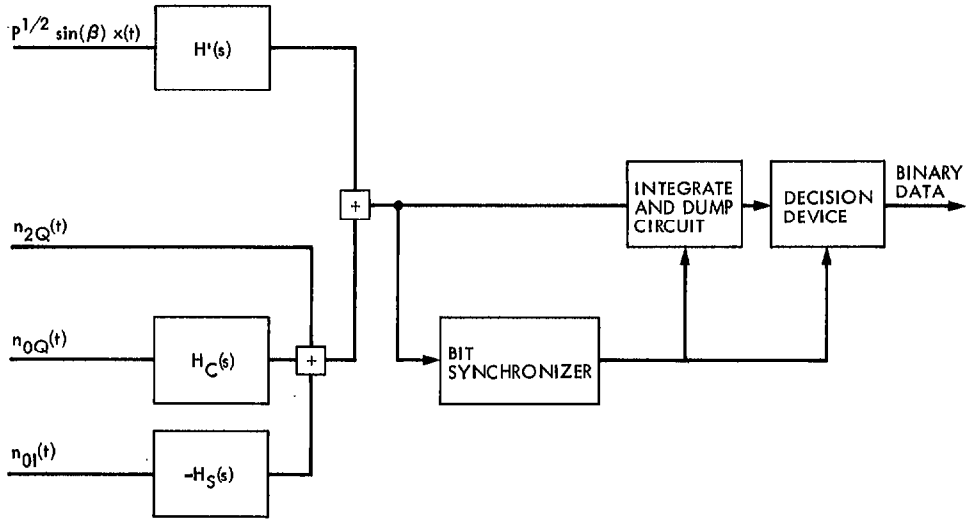

Fig. 3. A simplified analytical model for the DSN RF receiving system and telemetry detector

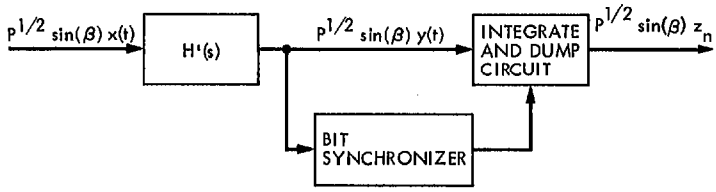

Fig. 4. Analytical model for determining the possible integrate-and-dump circuit output signal levels

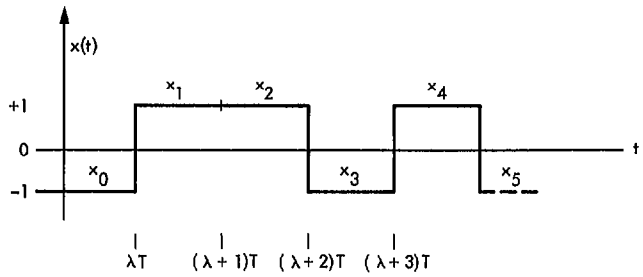

Fig. 5. Sample telemetry data signal *x(t)*

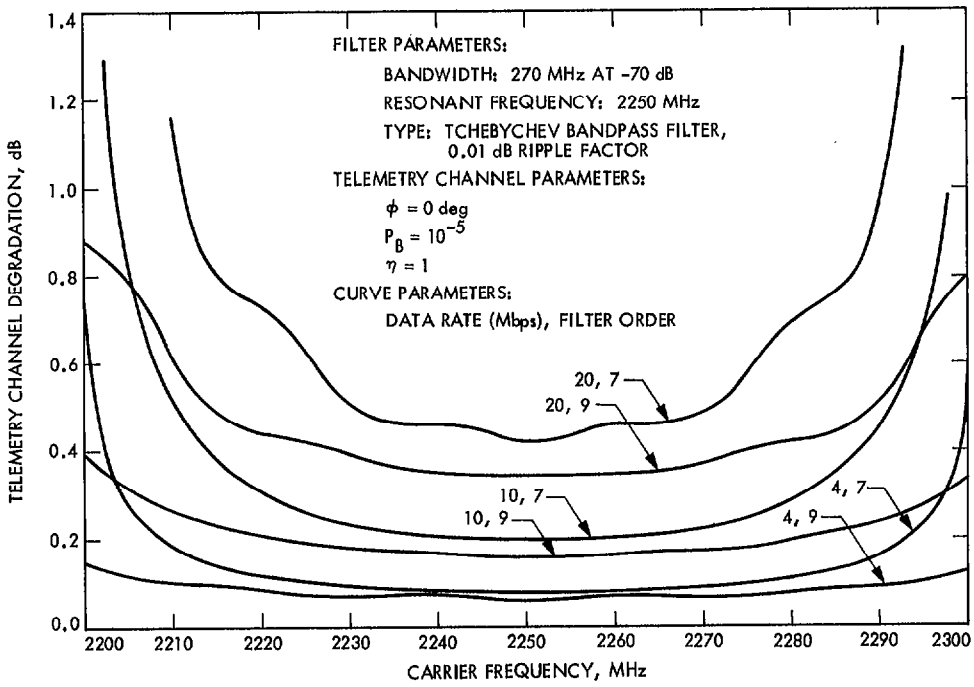

Fig. 6. Telemetry degradation as a function of carrier frequency for the S-band FET amplifier RFI filter assuming all noise originates after the RFI filter

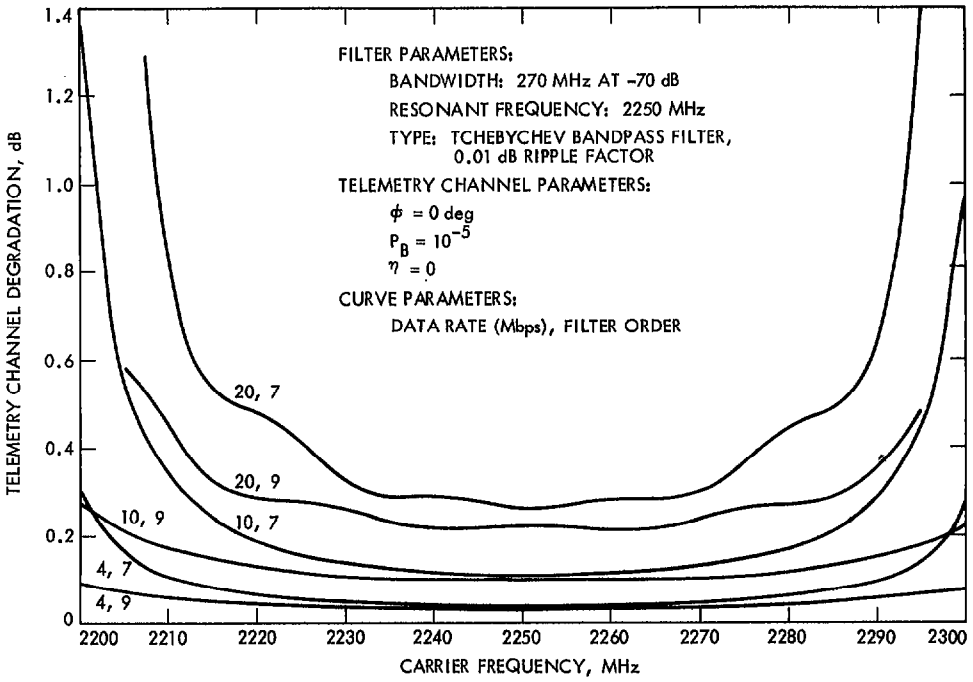

Fig. 7. Telemetry degradation as a function of carrier frequency for the S-band FET amplifier RFI filter assuming all noise originates before the RFI filter

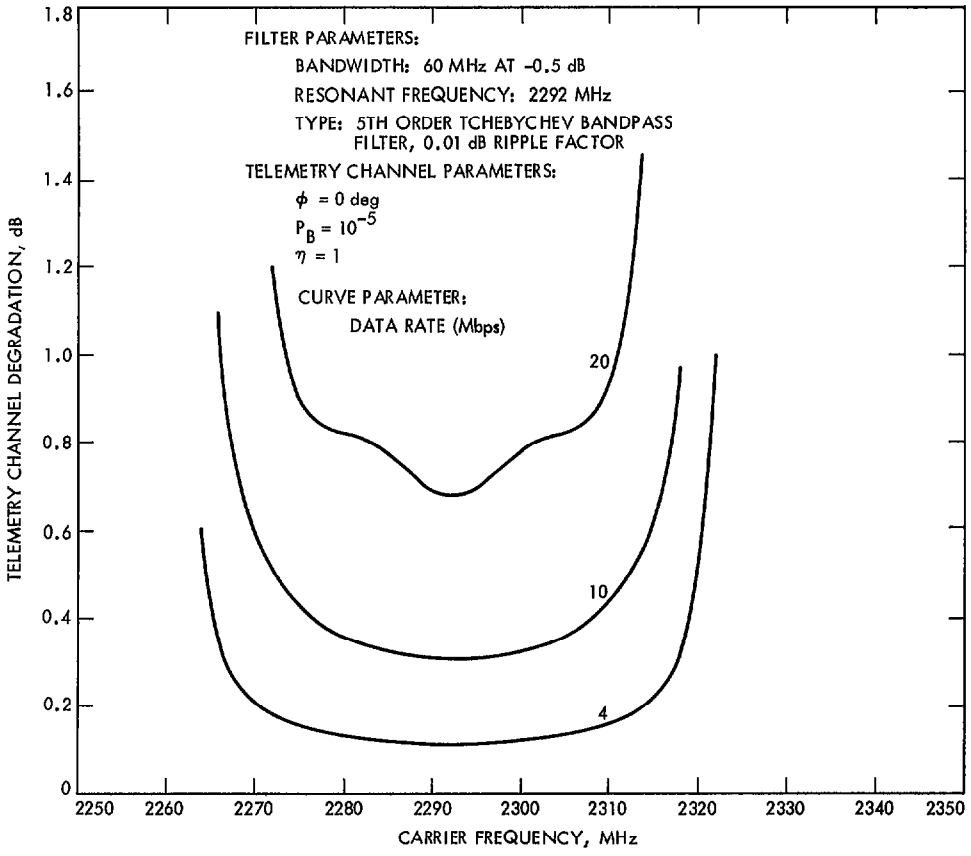

Fig. 8. Telemetry degradation as a function of carrier frequency for the S-band maser amplifier RFI filter assuming all noise originates after the RFI filter

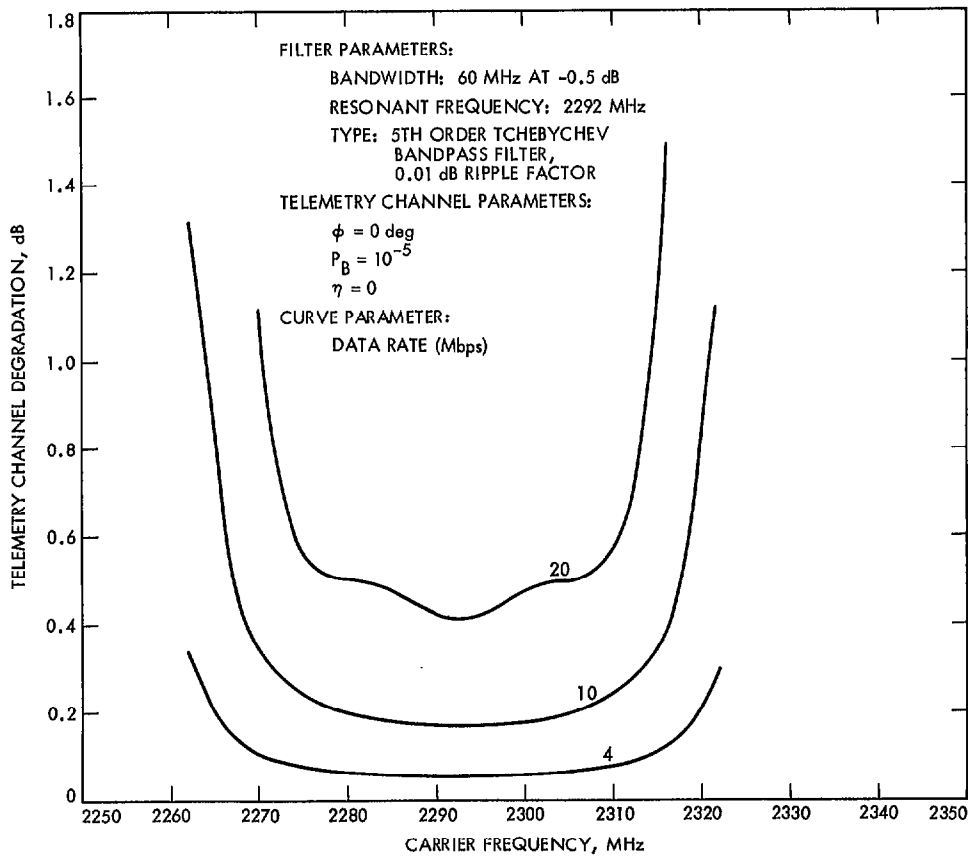

Fig. 9. Telemetry degradation as a function of carrier frequency for the S-band maser amplifier RFI filter assuming all noise originates before the RFI filter

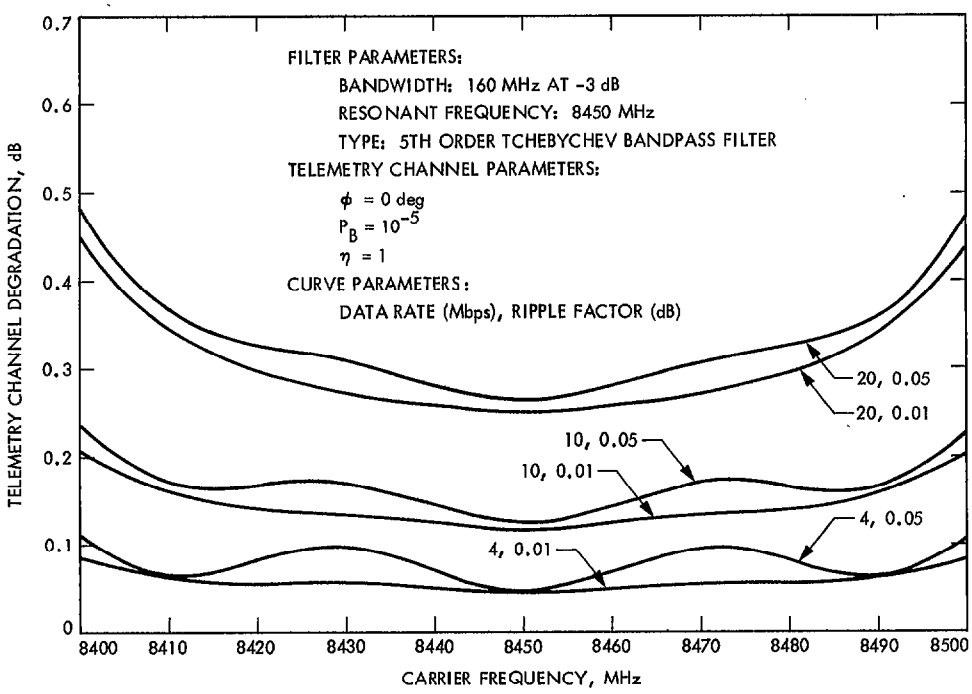

Fig. 10. Telemetry degradation as a function of carrier frequency for the X-band maser amplifier RFI filter assuming all noise originates after the RFI filter

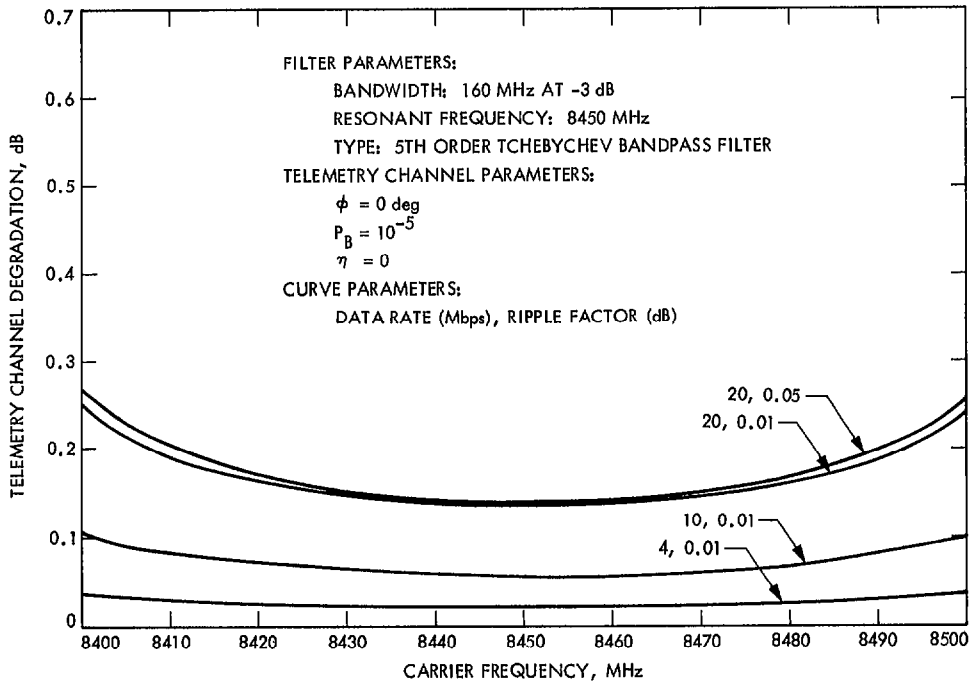

Fig. 11. Telemetry degradation as a function of carrier frequency for the X-band maser amplifier RFI filter assuming all noise originates before the RFI filter

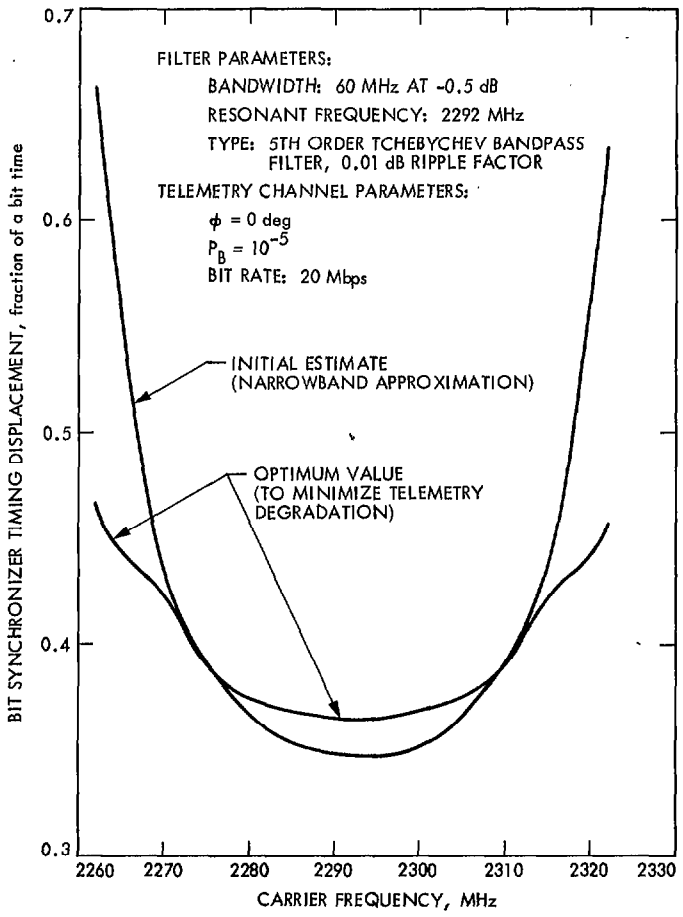

Fig. 12. Comparison of the initial estimate and optimum value of bit synchronizer timing displacement as a function of carrier frequency for the S-band maser amplifier RFI filter

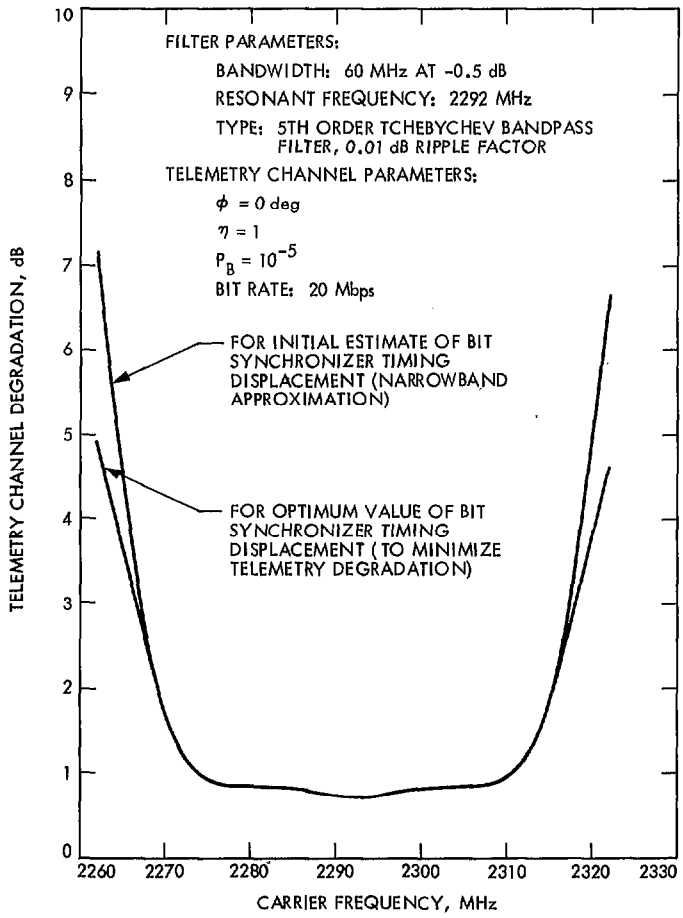

Fig. 13. Comparison of telemetry degradation as a function of carrier frequency for the initial estimate and optimum value of bit synchronizer timing displacement for the S-band maser amplifier RFI filter